Flight Software, Rigid Body, and Computational Fluid Dynamics Closed Loop Simulation

Martin I. Panevsky[1] and Barry J. Pataky[2]
The Aerospace Corporation, PO Box 92957, Los Angeles, CA 90009-2957

Phuong T. Than[3]
The Aerospace Corporation, PO Box 92957, Los Angeles, CA 90009-2957

A space vehicle simulation coupling a six degree of freedom (6DOF) rigid body model with computational fluid dynamics (CFD) models of the fuel and oxidizer has been created to simulate and assess the rigid body dynamics, fluid dynamics, and attitude control system performance. The coupled simulation is driven by the flight software and mission constants of the space vehicle. An overview of the method used to couple the 6DOF rigid body and CFD models is presented, as well as some of the algorithms used to solve the coupled rigid body and fluid equations of motion. A comparison between the simulation results and flight data show that the coupled simulation captures the main features of the fluid dynamics.

Nomenclature

dry rigid body	=	space vehicle excluding the fluid masses
rigid body	=	total space vehicle including the fluid mass as frozen mass
$F_{\text{propulsion}}$	=	vector of propulsion force acting on rigid body or dry rigid body
F_{fluid}	=	vector of force exerted by fluids on dry rigid body
I_{vehicle}	=	inertial tensor of rigid body about system center of mass
$I_{\text{dry rigid body}}$	=	inertial tensor of dry rigid body about system center of mass
m_{vehicle}	=	mass of rigid body
$m_{\text{dry rigid body}}$	=	mass of dry rigid body
ω	=	vector of angular velocity of rigid body or dry rigid body about system center of mass
$\dot{\omega}$	=	vector of angular acceleration of rigid body or dry rigid body about system center of mass
$M_{\text{propulsion}}$	=	vector of propulsion moments acting on rigid body
M_{fluid}	=	vector of fluid moments acting on dry rigid body
$\ddot{x}$	=	vector of linear acceleration of rigid body or dry rigid body
v	=	vector of linear velocity of rigid body or dry rigid body

I. Introduction

Fluid sloshing in launch vehicles and spacecraft is an area of considerable interest in the aerospace community. There were more than 1319 references in the literature dealing with slosh dynamics as of 2001[1]. As is well

[1] Senior Member of the Technical Staff, Flight Software Validation Department, M4/906
[2] Engineering Specialist, Flight Software Validation Department, M4/906
[3] Manager, Fluid Mechanical Analysis Section, Fluid Mechanics Department, M4/964

known, liquid sloshing in space vehicles can generate significant forces and moments through the fluid interaction with the tank walls and even affect the structural margins of the vehicle[2]. Fuel and oxidizer dynamics affect the stability and control of the space vehicle, the propellant budget of the attitude control system, as well as the design of the vehicle flight software[3, 4, 5]. Since the flight program controls all aspects of the space vehicle's performance, testing and validating the flight code invariably leads to a comprehensive assessment of the various vehicle subsystems. This requires a simulation environment incorporating the flight software and a realistic simulation of the space vehicle tightly coupled in a closed-loop system. Over the years, there have been numerous attempts to model the slosh dynamics either analytically or numerically. Analytical solutions usually use a simplified mechanical pendulum analogy which allows the integration of the fluid model into a comprehensive dynamical model of the space vehicle[4, 6, 7]. A drawback of this approach is its low fidelity, especially in a low-G environment. Another approach attempts to cast the rigid body dynamics and the fluid dynamics as a finite element problem[8-9]. This incurs an enormous computational load on the simulation. Moreover, the available simulation tools are generally designed as stand-alone software packages pertaining to either a structures and dynamics paradigm or a strictly fluid dynamics paradigm. This necessitates extensive and potentially difficult customization efforts in creating an integrated approach. In our work the space vehicle is described as a composite system consisting of a dry rigid body and several fluid masses. We are leveraging the speed and fidelity of a traditional six degree of freedom rigid body dynamics simulation to model the dynamics of the dry space vehicle and an off-the-shelf computational fluid dynamics software package to model the fluid dynamics. We present a simulation that couples the fluid dynamics with the dry rigid body dynamics while driven by the flight code and mission constants of the space vehicle.

II. Overview of the Coupled Rigid-Body – Fluid Dynamics Simulation

A 6DOF rigid body simulation models the space vehicle and provides simulated sensor input to the flight code as it executes its guidance, navigation, and sequencing algorithms in flight mode. The time step of the entire simulation is determined by the time step of the flight code. If the fluid time step required for scheme stability (Courant–Friedrichs–Lewy condition) is smaller than the flight time step, then interpolation is used to determine the fluid condition within that time step. If the fluid time step is greater than the flight time step, a smaller time step of about half of the flight time step is enforced. Such restriction ensures the fluid dynamics state is always interpolated and not extrapolated.

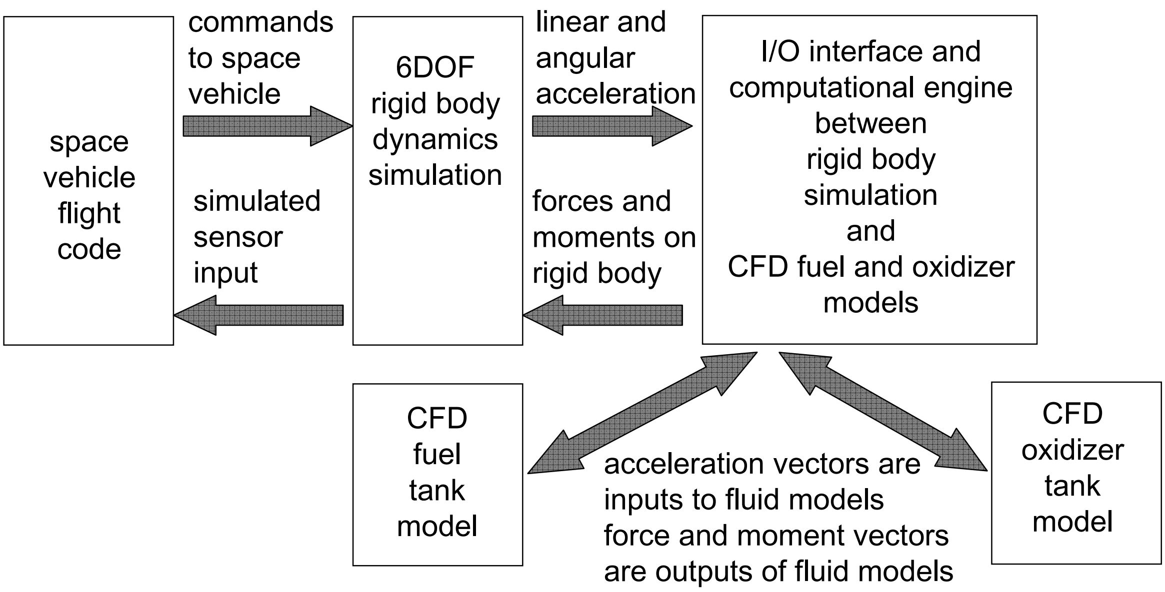

Figure 1. Logic flow diagram. *The simulation loop couples the flight code, the rigid body dynamics model, and the computational fluid dynamics models of the fuel and oxidizer.*

The interface between the rigid body dynamics simulation and the CFD models is implemented as an iterative numerical method. At the beginning of every time step the flight software issues commands to the space vehicle and the simulation calculates the linear and angular accelerations of the total space vehicle as a rigid body. Angular accelerations are integrated to obtain the angular velocities and together with the linear accelerations, they are used as inputs to generate the CFD solutions in the vehicle body frame. Outputs of the CFD solutions are fluid forces and moments acting on the tank walls about the vehicle's center of mass. These forces and moments are combined with other external forces and moments generated by the propulsion system, aerodynamics, etc. The simulation then performs an iterative step of re-evaluating the linear and angular accelerations on the rigid body. In this step the rigid body equations of motion are those for a dry rigid body, which is the space vehicle excluding the fuel and oxidizer masses. The forces and moments generated by the fluid dynamics are treated as external forces and moments in the translational and rotational equations of motion of the dry rigid body. After the linear and angular accelerations are re-evaluated, the rigid body simulation integrates them and generates the CFD-corrected sensor inputs to the flight software. This closes the integration loop and starts a new time step. Figure 1 gives a broad overview of the coupled simulation architecture. A more detailed description of the integration algorithm will be given in the next section.

III. Integration Algorithm

The algorithm described here is adaptable to various simulations as it uses physical quantities that are common to both rigid body dynamics and CFD models. At the same time, the rigid body simulation can be expanded to incorporate additional simulation modules and modified to describe various space vehicles without affecting the functionality of the interface algorithm. Before providing the details of the rigid body dynamics algorithm, a brief description of the fluid dynamics is given.

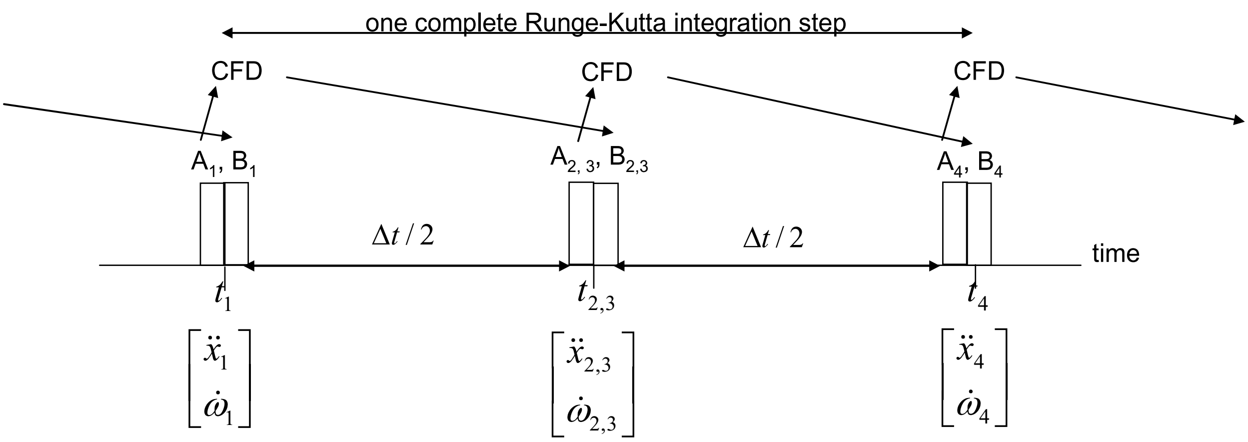

Figure 2. Interface algorithm. *The fourth-order Runge-Kutta integrator evaluates the linear acceleration* $\ddot{x}$ *and the angular acceleration* $\dot{\omega}$ *at four intermediate time points within a main time step of the simulation. At every* A_i *time point the initial step is run and at every* B_i *time point the iterative step is run. The integrands are shown in square brackets.*

The propulsion system of the space vehicle uses a bi-propellant system, fuel and oxidizer, whose tank geometry shares a common shape. The tanks consist of a cylindrical section whose ends connect to two hemispheres and are partially filled with propellant. FLOW3D of Flow Science Inc. was used to compute the fluid dynamics. Propellant is assumed to behave like a viscous, incompressible Newtonian fluid. Flow solutions also account for the effect of surface tension, which is expected to influence the gas-liquid interface at and near the solid boundaries in the low gravity environment. Solutions are computed on a non-inertial frame with the observer being fixed with the tank coordinates, and have a first order accuracy in both time and space.

The fuel tank has 811,000 cells and the oxidizer 730,000 cells; both have uniform cell spacing. No-slip boundary conditions were imposed on all solid boundaries. The tank ullage is not modeled in the computation so its pressure was taken to be zero. This has no effect on the fluid dynamics since the fuel and oxidizer are treated as incompressible. The presence of surface tension requires the contact angle be prescribed on solid surfaces and is assumed zero for these simulations.

The rigid body simulation uses a fourth-order Runge-Kutta (RK4) method to integrate the equations of motion. The interaction of the RK4 and CFD codes is shown in Figure 2. For each Δt step the integrator computes linear and angular accelerations of the rigid body at times t, $t+\Delta t/2$, and $t+\Delta t$, and it interacts with the CFD solver at these times in order to produce the final linear and angular accelerations of the dry rigid body. Having evaluated the accelerations at these intermediate points, the RK4 algorithm integrates and produces the linear and angular velocities of the dry rigid body at time $t+\Delta t$. A typical iterative cycle at some time t_i starts by computing the linear and angular accelerations of the rigid body using the equations of motion Eq. (1a) and Eq. (1b):

$$m_{\text{vehicle}}\ddot{x} + m_{\text{vehicle}}\omega \times v = F_{\text{propulsion}} \tag{1a}$$

$$\dot{\omega} = I_{\text{vehicle}}^{-1}(M_{\text{prop}} - \omega \times (I_{\text{vehicle}}\omega)) \tag{1b}$$

The angular velocity ω and the propulsion moments M_{prop} in the above equations are resolved in the body-fixed frame. In this rigid-body-only phase of the coupling algorithm the vehicle mass m_{vehicle} is the total mass of the space vehicle and the fluid forces and moments on the tanks are considered internal and do not enter the equations of motion. The resulting linear and angular accelerations are then passed as inputs to the CFD models of the fuel and oxidizer. These accelerations represent the tank accelerations at time t_i. The CFD algorithm computes the new fluid forces and moments at time $t_i + \Delta t/2$ in preparation for the next iterative step at time $t_i + \Delta t/2$. The maximum time step of the fluid solver is set at $\Delta t/2$ but within that time step the CFD solver is free to make smaller intermediate time steps in order to satisfy its internal convergence criteria. The coupling algorithm then executes its iterative step for t_i by summing the fluid forces and moments with the propulsion, aerodynamic, etc. forces and moments and applying them to the dry rigid body of the space vehicle. The fluid forces and moments enter into the equations of motion as shown in Eq. (2a) and Eq. (2b):

$$F_{\text{propulsion}} + F_{\text{fluid}} = m_{\text{dry rigid body}}\ddot{x} + m_{\text{dry rigid body}}\omega \times v \tag{2a}$$

$$M_{\text{propulsion}} + M_{\text{fluid}} = I_{\text{dry rigid body}}\dot{\omega} + \omega \times (I_{\text{dry rigid body}}\omega) \tag{2b}$$

In applying Eqs. (2a) and (2b) it is important to note that the dry rigid body is rotating about the center of gravity of the composite mass system consisting of the dry rigid body and the fluid masses. Consequently, the inertial tensor $I_{\text{dry rigid body}}$ is computed about that point. Equations (2a) and (2b) are used to evaluate the CFD-modified $\ddot{x}$ and $\dot{\omega}$. The coupling algorithm implies a phase offset of $\Delta t/2$ between the rigid body model and the CFD model. This timing offset is much smaller than the characteristic time scale of the fluid dynamics and its influence on the overall fidelity is negligible. On the other hand, the iterative cycle greatly improves the numerical stability of the coupling algorithm. As the following plots and discussion illustrate, the coupled rigid-body – CFD simulation provides an improved accuracy over a rigid-body-only simulation when compared to flight data. For simulations where an even greater numerical accuracy is needed, the coupled simulation allows multiple rigid-body – CFD iterations on the same time step. Ongoing work to further increase the simulation precision will be discussed in the next section.

IV. Simulation Results and Discussion

We compare the simulation results with the flight data of a space vehicle to evaluate the fidelity of the coupled simulation. Fluid dynamics effects on the attitude control of the space vehicle are identified by comparing the results to a baseline case in which the fluid is assumed to move rigidly with the space vehicle. Figure 3 provides a time history plot of the normalized roll, pitch, and yaw rates of the space vehicle. The body rates of the space vehicle are a good measure of the characteristics of fluid slosh as they reflect the interaction between the fluid dynamics and the attitude control system as it tries to maintain the space vehicle within a certain pointing error. The chosen flight segment is such that the perturbations of the body rates from the baseline case are due to slosh. The initial time segment from 0 sec to 500 sec of Figure 3 is characterized by a constant roll phase with axial settling applied. The roll creates a surface slosh wave with the fluid rotating in the tank. In the second time segment from 500 sec to 1000 sec of Figure 3 the space vehicle is actively maneuvering.

Figure 3 shows that the coupled simulation captures the main features of the fluid dynamics better than the rigid-body-only simulation. These features include the timing, duration, amplitude, and frequency content of the vehicle angular rates in all three axes as the vehicle is maneuvering from 500 sec to 1000 sec. The maximum phase difference between the slosh dynamics in the flight data and in the coupled simulation is about 10% of the slosh period and is likely due to different initial conditions. The pitch and yaw plots indicate that the coupled simulation captures the wavelike disturbance from 500 sec to 750 sec that the rotating fluid slosh exerts on the space vehicle. In addition, the fluid-induced disturbances in the pitch and yaw axes for the same time period have a phase offset of approximately 90 degrees which agrees with the expected fluid slosh of a rotating surface wave. The comparison with the flight data indicates that the new rigid-body – CFD simulation is an improvement over the rigid-body simulation approach since the rigid-body-only simulation does not have the capability to predict any of the observed fluid-induced effects on the body rates. The pitch rate discrepancy at 500 sec is due to a phase offset between the simulated fluid dynamics and the fluid dynamics reconstructed from the flight data.

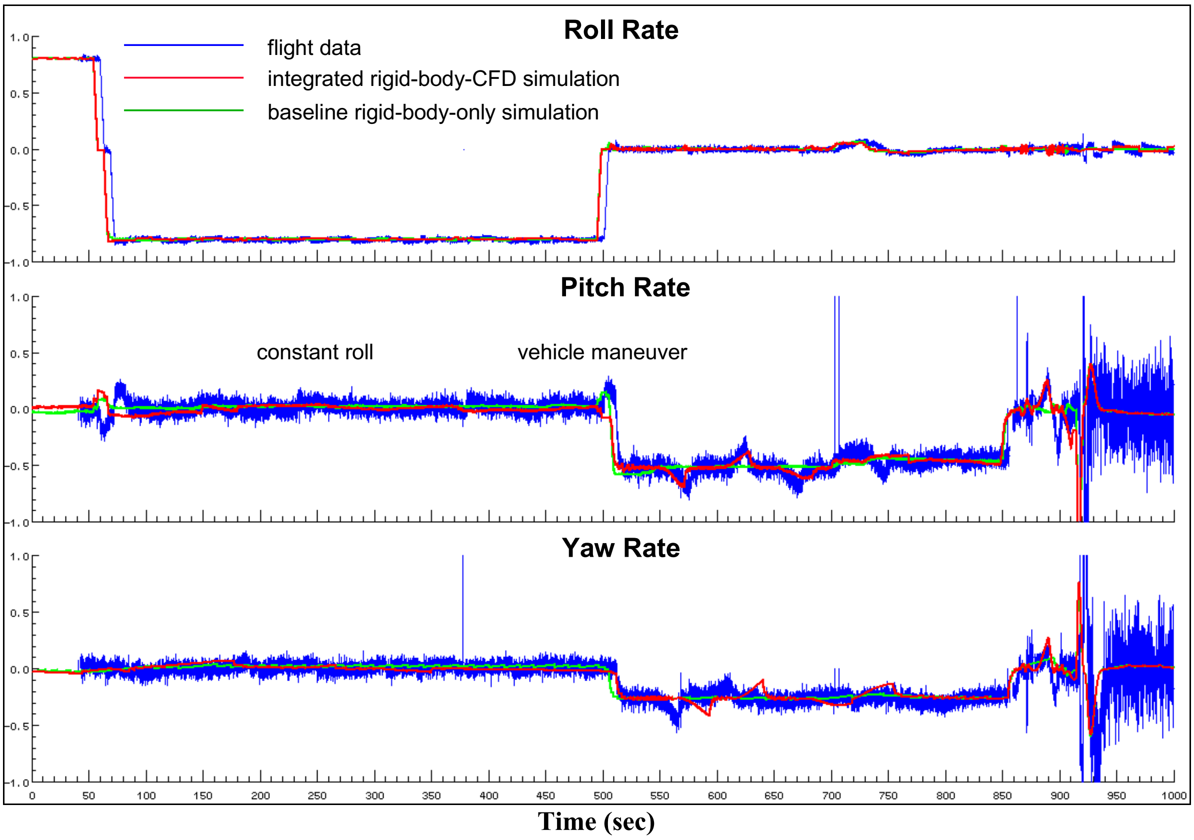

Figure 3. Normalized roll, pitch, and yaw rates caused by fluid slosh (Vehicle maneuvering). *Flight data is compared to results from the coupled rigid-body-CFD simulation. The rigid-body-only simulation is used as a baseline. The spikes in the flight data are telemetry dropouts.*

Figure 4 shows another time segment of the flight characterized by fluid slosh. This also is a time history plot of the normalized roll, pitch, and yaw rates of the space vehicle. In this time segment the fluid slosh is initialized by a roll disturbance.

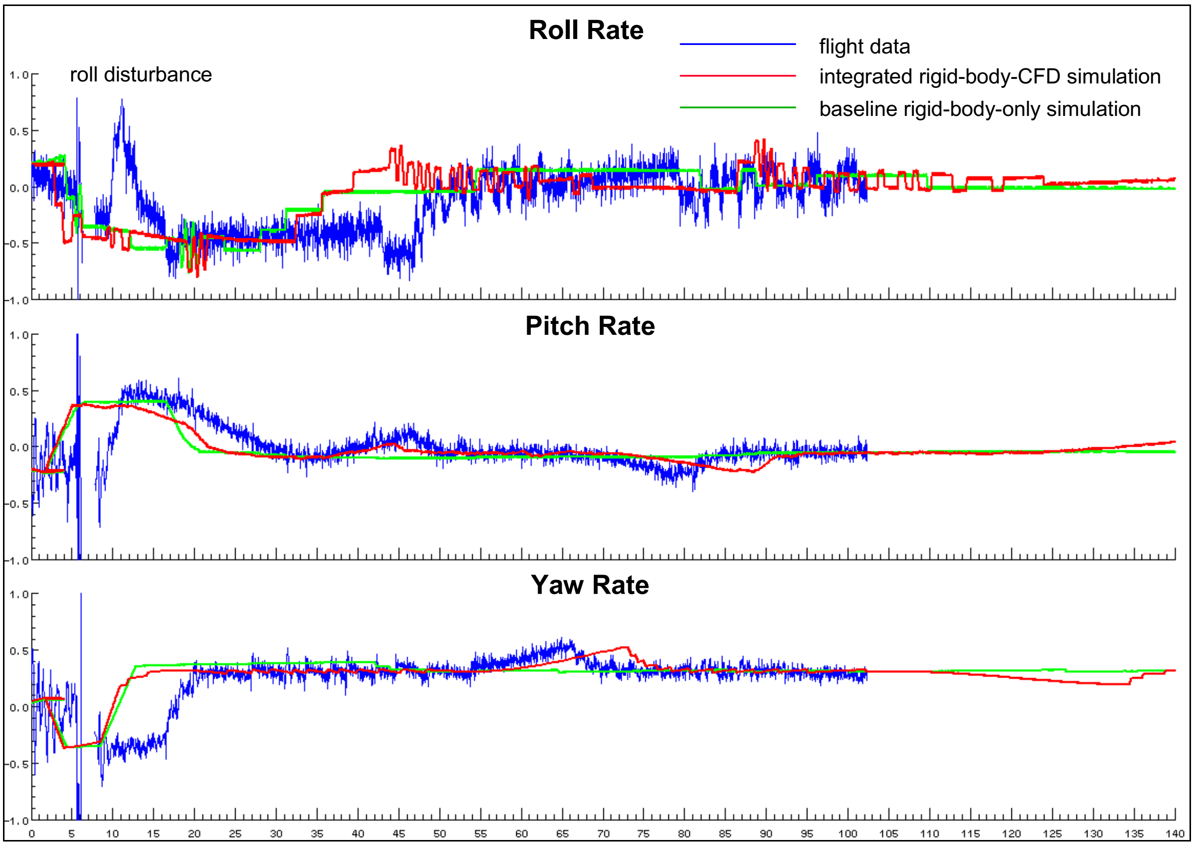

Figure 4. Normalized roll, pitch, and yaw rates caused by fluid slosh (Roll disturbance). *Flight data is compared to results from the coupled rigid-body-CFD simulation. The rigid-body-only simulation is used as a baseline.*

The roll disturbance impulse along the roll axis of the space vehicle was not modeled in the rigid-body simulation. As a result, the effect from this disturbance was not captured in the CFD simulations. This accounts for the discrepancy between the roll, pitch, and yaw rates of both simulations and the flight data at the beginning of this time segment. It also explains the phase bias between the fluid effects predicted by the coupled simulation and the flight data. Figure 4 shows that as the attitude control system settles the fluid, the interaction between the dry rigid body and the fluid allows the coupled simulation, after a transient period, to track the main features of the fluid slosh on the space vehicle. As in Figure 3, the pitch and yaw rates exhibit the characteristic wavelike pattern of a rotating fluid slosh. The simulated pitch and yaw rates closely approximate the observed timing, duration, amplitude, and frequency content of the fluid motion. The quarter-period phase offset between the fluid-induced pitch and yaw rates agrees with the expected phase delay for a rotating fluid. The coupled rigid-body – CFD simulation proceeds beyond the flight data dropout at time 102 sec, continuing to predict the fluid dynamics effects on the space vehicle's attitude rates.

The flight data dropout illustrates the predictive value of the coupled rigid-body – CFD simulation in Figure 5. Besides the additional demands that fluid slosh places on the vehicle structure, sloshing also affects the vehicle attitude control system and associated propellants. This is an important consideration in the overall design and performance of the space vehicle and an area where an accurate prediction of the fluid dynamics is beneficial. Figure

5 presents a dimensionless plot of the attitude control system propellant usage during the period of flight segment under consideration. We compare the simulated attitude control system propellant usage with the actual usage reconstructed from flight data. We include the results from the baseline case of a rigid-body-only simulation to demonstrate the need to include the fluid dynamics effects. In Figure 5, both the rigid-body-only simulation and the coupled rigid-body – CFD simulation start this flight segment at identical levels of the attitude control system propellant. The coupled simulation accurately tracks the propellant usage, while the rigid-body-only simulation diverges from the true value. After the telemetry data stream is restored, the coupled simulation continues to closely approximate the true value of propellant usage. The divergence between the two simulations becomes more pronounced at the end of the shown flight segment which corresponds to the vehicle maneuvering. While the vehicle is reorienting, the increased fluid slosh results in a higher rate of propellant usage by the attitude control system. The coupled rigid-body – CFD simulation captures that additional dynamics while the rigid-body-only simulation completely misses it.

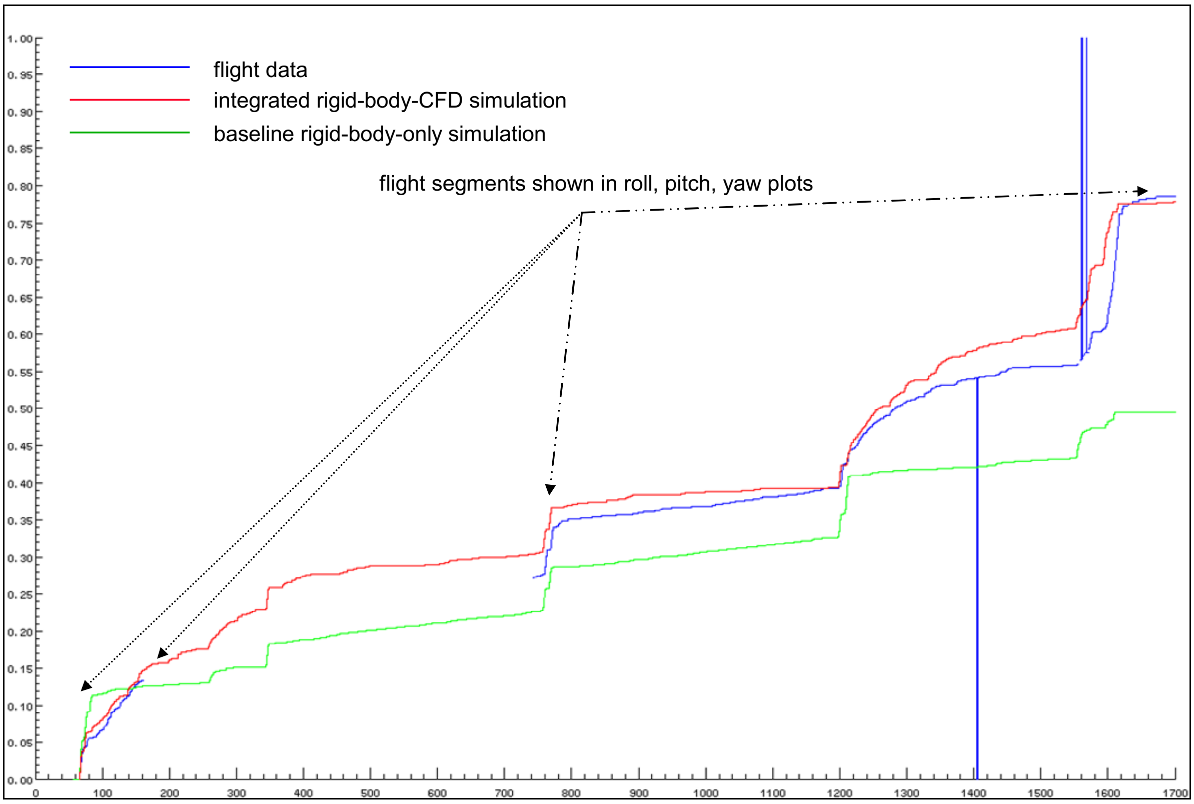

Figure 5. Normalized attitude control system propellant usage. *Flight data is compared to results from the combined rigid body-CFD simulation. The rigid body-only simulation is used as a baseline. The spikes in the flight data are telemetry dropouts.*

Work is under way to further improve the fidelity of the integration algorithm and the speed of the fluid model. The enhancement will focus on improving the iterative method by removing the assumption that the fluid moves rigidly with the space vehicle in the rigid-body phase of the coupling algorithm. Instead, the goal is to use a dry-rigid-body approach for all steps of the coupling algorithm and to allow for multiple iterations and convergence checking on the same time step. Another improvement is the incorporation of a moving center of mass in the integration algorithm. The fluid sloshing causes slight shifting of the center of mass of the composite rigid body–fluid mass system. The enhanced integration algorithm will then be applicable to space systems that exhibit violent fluid slosh resulting in a temporary loss of contact between the fluid and the tank walls. Another upgrade to the simulation is the creation of a highly parallel environment for the execution of the fluid models with the accompanying reduction in simulation runtime. The parallel execution of the CFD solver will also allow us to increase the level of detail and fidelity of the fluid and tank models without unduly increasing the execution runtime.

V. Conclusions

We have presented a numerical algorithm that combines a 6DOF dynamics simulation, a CFD model, and the flight code of a space vehicle into a closed loop simulation. A comparison between the simulation results and flight data indicates that the simulation captures the main features of the fluid dynamics. The proposed algorithm has demonstrated stability and accuracy in modeling the interaction between the rigid body dynamics and the fluid motion. The fidelity of the coupled approach allows precise analysis of the propellant and payload budget of the space vehicle and the performance of the attitude control system under various flight configurations. In the case of a spacecraft, attitude control is strongly affected by fluid slosh. Therefore, the ability to model, predict, and analyze slosh is an important consideration. In addition, the ability of the rigid-body – CFD simulation to accurately estimate the propellant budget has a direct bearing on the projected lifespan of the spacecraft. Such an approach increases the accuracy of predicting the performance of space vehicles, thus reducing the risk of a mission failure.

VI. Acknowledgements

The authors wish to extend gratitude to Darrell D. Gritz for supporting the project, to Khoi D. Le for processing the flight data, and to the Aerospace reviewers Martin M. Tong, Jo-Lien Yang, and Michael A. Weaver for many constructive suggestions and valuable advice.

References

[1]Ibrahim, R. A., Pilipchuk, V. N, Ikeda, T., "Recent Advances in Liquid Sloshing Dynamics," *Applied Mechanics Review*, Vol. 54, No. 2, 2001, pp. 133-199.

[2]Navickas, J., Cheng, P., "Effect of Propellant Sloshing on the Design of Space Vehicle Propellant Storage Systems," *Proceedings of the AIAA/SAE/ASME/ASEE 26th Joint Propulsion Conference*, Orlando, FL, 1990.

[3]Saugen, J. D., "Adaptive Control of Propellant Slosh for a Launch Vehicle with Multiple Tanks," *Proceedings of the AIAA Guidance, Navigation, and Control Conference*, Vol. 3, New Orleans, LA, 1991, pp. 1833-1842.

[4]Bayle, O., L'Hullier, V., Ganet, M., Delpy, P., Francart, J. L., Paris, D., "Influence of the ATV Propellant Sloshing on the GNC Performance", *Proceedings of the AIAA Guidance, Navigation, and Control Conference and Exhibit,* Monterey, CA, 2002.

[5]Wie, B., "Thrust Vector Control Design for a Liquid Upper Stage Spacecraft", *Journal of Guidance, Control, and Dynamics,* Vol. 8, No. 5, 1985, pp. 566-572.

[6]Enright, P. J., Wong, E. C., "Propellant Slosh Models for the Cassini spacecraft," *Proceedings of the AIAA/AAS Astrodynamics Conference*, Scottsdale, AZ, 1994, pp. 186-195.

[7]Kana, D. D., "A Model for Nonlinear Rotary Slosh in Propellant Tanks," *Journal of Spacecraft and Rockets*, Vol. 24, No. 2, 1987, pp. 169-177.

[8]Kim, M. C., Lee, S. S., Kabe, A. M., "Consistent and Lumped Area Formulations in Fluid-structure Interaction", *Proceedings of the* 38th *AIAA/ASME/ASCE/AHS/ASC Structures, Structural Dynamics, and Materials Conference and Exhibit, and AIAA/ASME/AHS Adaptive Structures Forum* , Kissimmee, FL, 1997, Collection of Technical Papers, Pt. 1.

[9]Lowry, S. A., Yang, H. Q., LaLanne, R., "Design Optimization of the STS External LOX tank using a coupled fluid-structures dynamics code with free surface tracking," *Proceedings of the 34th Aerospace Sciences Meeting and Exhibit,* Reno, NV, 1996.